A STUDY OF GAS SOLUBILITIES AND TRANSPORT
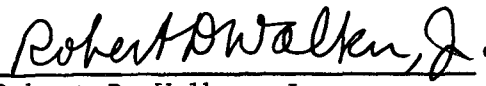PROPERTIES IN FUEL CELL ELECTROLYTES

Research Grant NGR 10-005-022

Third Semi-Annual Report

Period Covered: September 1, 1966 - February 28, 1967

Prepared For

National Aeronautics and Space Administration

Washington, D. C.

March 29, 1967

Robert D. Walker, Jr.
Principal Investigator

ENGINEERING AND INDUSTRIAL EXPERIMENT STATION

College of Engineering
University of Florida
Gainesville, Florida

TABLE OF CONTENTS

i

LIST OF TABLES

LIST OF FIGURES

iii

ABSTRACT

Work described in this report covered (1) density measurements, (2) correlation of vapor pressures, (3) measurements of the solubility of oxygen in KOH solutions, and (4) measurements of the mutual diffusivity of water in KOH.

By means of a modified Westphal balance technique using a silver plummet, measurements of the density of aqueous KOH solutions have been made up to a temperature of $161.4^{\circ}C$ and a KOH concentration of 77.1 wt. %. Good agreement with previously published data was noted.

Vapor pressures of KOH solutions were correlated by means of the Antoine equations using a digital computer for evaluation of the constants. It was found that the data were best represented at each concentration by one equation for low temperatures and another equation for high temperatures. The transition temperature from the low to the high temperature region increased with KOH concentration. Predicted vapor pressures using the constants so determined agreed with experimental values within one percent.

Oxygen solubilities were extended to $100^{\circ}C$ and a KOH concentration of 56 wt. % after refining the technique. The present technique is limited to the range indicated by impurities in the helium used as a stripping gas. Further imprpvements in the apparatus and technique are being investigated to permit extension of the measurements to higher temperatures and KOH concentrations.

Measurements of the mutual diffusivity of water in aqueous KOH solutions have been started and a few data are reported.

1

1.0 Introduction

The past six months have been utilized almost entirely in determining needed physical data and in further refining methods of analysis. At the beginning of the period it appeared that the method of measuring dissolved oxygen concentrations was adequate. It was soon found, however, that the solubility of oxygen in concentrated KOH solutions, especially at high temperatures, was so small that unacceptably large errors were being noted. This was the more serious in that diffusivity measurements depended on making measurements in solutions which were not saturated with oxygen. It was necessary, therefore, to reduce these errors to an acceptable value. This has been accomplished, and measurements of solubility up to $100^{\circ}C$ carried out.

Measurements of the density of KOH solutions have been extended to $160^{\circ}C$, and vapor pressures of KOH solutions correlated by means of the Antoine equation over the range of temperatures and KOH concentrations of chief interest for H_2-O_2 fuel cells employing aqueous KOH solutions as electrolytes.

In the course of this investigation it became evident that a knowledge of the mutual diffusivity of water in KOH solutions is desirable for a more adequate understanding of mass transport in these solutions. To that end measurements of the mutual diffusivity were begun. A few of these data are reported here.

2

2.0 DENSITY MEASUREMENT

Considerable difficulties were experienced with the pycnometer procedure described in the previous report when making measurements at high temperature. These difficulties arose primarily from rapid corrosion of the glass capillary. In view of these problems a modified Westphal balance procedure (Hydrostatic Weighing Method of Kohlrausch) has been adopted and is described below.

Theory. This method is based on the Archimedes Principle, in which a plummet is weighed in air, water, and the solution whose density is to be determined, respectively. The density of the solution at the temperature t_1, at which this measurement is conducted is given by

$$\rho_{soln} = \left(\frac{W_S - W_A}{W_W - W_A} \right) \times \rho_{water\ at\ t_i} \qquad (2.0\text{-}1)$$

where W_S = weight of the plummet in the solution

W_A = weight of the plummet in air

W_W = weight of the plummet in water.

Using this method Reddlich and Bigeleisen (1), who used a plummet having a volume of 300cc, claimed that under optimum conditions, the reproducibility of density measurement can be as high as $\pm 2.0 \times 10^{-6}$ gm/cc.

Description of Apparatus.

An analytical balance with one pan replaced by a coin silver plummet (approximately 5 cc in volume) suspended by a fine Platinum-Rhodium wire was used. The wire passed through a hole (about 3/8" in diameter) in the platform of the balance so that the plummet could be immersed in thermostated potassium hydroxide solution placed below the balance case. To prevent corrosion of the plummet it was electroplated

with pure silver.

To prevent evaporation from the KOH solution being tested a
flow of nitrogen equilibrated with KOH of the same concentration and at
the same temperature as the sample under test was directed over the
surface of the solution. To accomplish this two groups of saturators
were used as shown in Figure 1. The first group consisted of two
saturators containing distilled water kept at a temperture such that
the vapor pressure of water is the same as that of the KOH solution.
The second group consisted of two more saturators at the same tempera-
ture and KOH concentration as that of the sample.

Procedure.

The plummet was weighed first in air and then in the KOH solu-
tion which was maintained at a fixed temperature. The plummet was im-
mersed to such a depth that the surface of the solution always came to
the same mark on the wire, so that the same volume of liquid was dis-
placed at all times. Then the weight of the plummet was determined at
intervals of 5 minutes, to ensure that an equilibrium condition was
reached and to guard against accidental errors in weighing. The temp-
erature of the solution was determined at the beginning and the end of
each experiment. The experiment was repeated three to five times with
fresh samples of the same composition to ensure reproducibility.

The plummet volume for temperatures up to $80^{\circ}C$ was determined
by weighing the plummet in water in the same manner as stated above.
For temperatures above $80^{\circ}C$, the volume of the plummet was obtained by
extrapolating that obtained at lower temperature to the desired tempera-
ture, assuming that the thermal expansion coefficient of silver remains
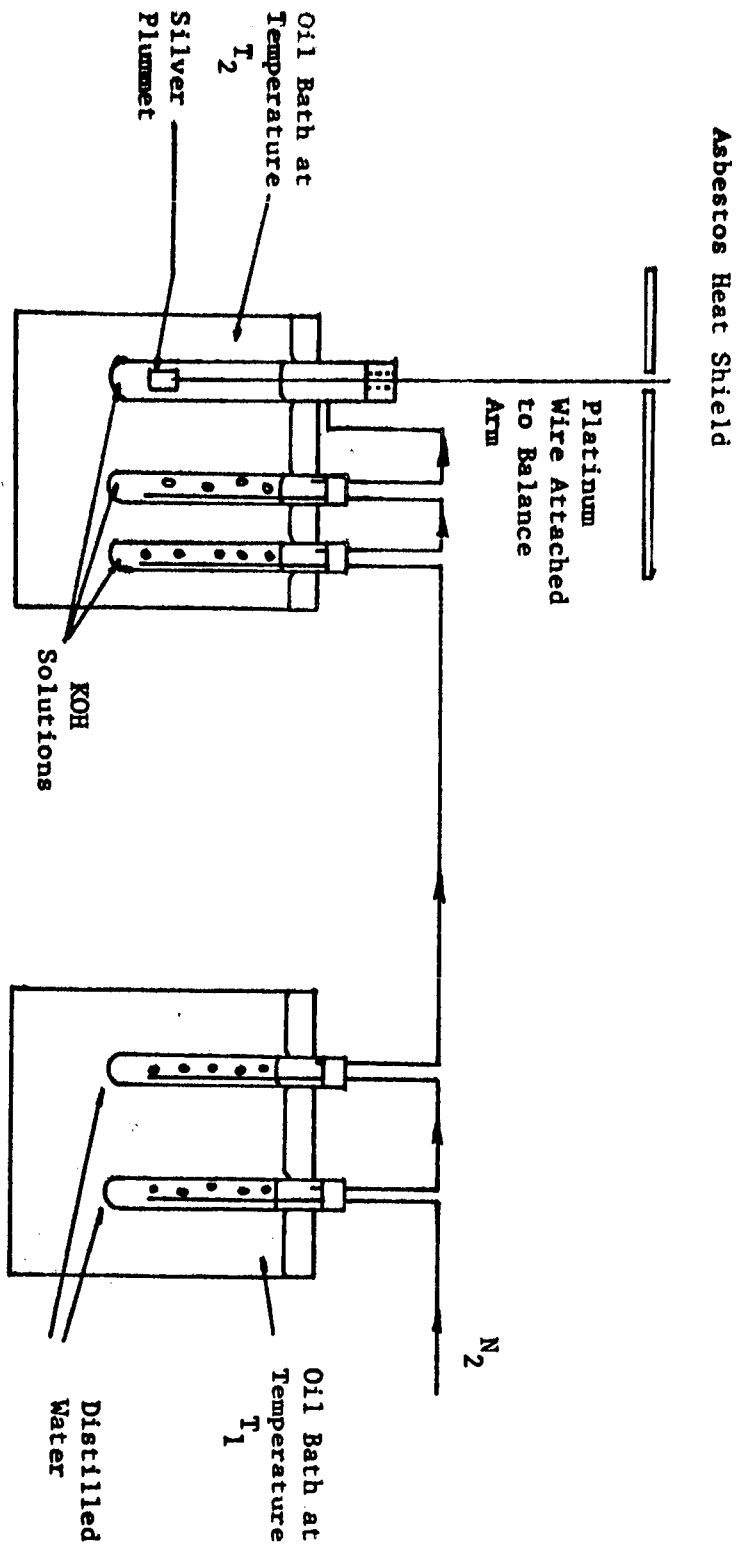
Figure 1

SATURATORS FOR DENSITY MEASUREMENTS

constant over the interval of $80^{o}C$ to $160^{o}C$. At $80^{o}C$ the volumetric expansion coefficient was approximately $0.00006(^{o}C)^{-1}$.

At high temperature, the solution tended to vaporize quite rapidly, thus affecting the temperature and concentration of the solution. To minimize this effect, an atmosphere of nitrogen saturated with water vapor was maintained by passing presaturated nitrogen over the surface.

In experimenting with dilute solutions, dissolved gas in the solution tended to form small bubbles and adhere to the surface of the plummet, and had to be removed before taking readings.

Concentrated solutions, whose saturation temperatures are above room temperature, were prepared and stored in an oven maintained at temperatures higher than the saturation temperature, and the concentration was determined at the time of density measurement by titration.

Note: In these experiments, no attempt was made to free the potassium hydroxide solution of carbonate, but the carbonate content for each concentration was determined and was found to be less than one per cent of the potassium hydroxide content. Also, no attempt was made to eliminate the effect of surface tension by coating the wire with platinum black.

Discussion of Results.

The densities of potassium hydroxide solutions at various temperatures and concentrations are tabulated in Table 2.0-1 and are shown in Figures 2 and 3. These results agree closely with the data from Table 5 of Solvay Technical Bulletin No. 15 for $60^{o}C$ and $80^{o}C$. The

Table 2.0-1

DENSITIES OF KOH SOLUTIONS

Wt. percent KOH	59.9 ± 0.1°C		79.9 ± 0.1°C	
	Exptl. Data	Solvay Data	Exptl. Data	Solvay Data
6.17	1.0381 ± 0.0001	1.0375	1.0269 ± 0.0001	1.0279
11.50	1.0863 ± 0.0002	1.0857	1.0746 ± 0.0001	1.0767
20.90	1.1758 ± 0.0002	1.1750	1.1652 ± 0.0001	1.1650
27.80	1.2448 ± 0.0001	1.2441	1.2329 ± 0.0001	1.2336
36.00	1.3294 ± 0.0002	1.3299	1.3973 ± 0.0001	1.3955
43.00	1.4080 ± 0.0001	1.4072	1.3180 ± 0.0001	1.3186
47.20	1.4560 ± 0.0001	1.4554	1.4442 ± 0.0008	1.4435
50.37	1.4957 ± 0.0001	1.4925[*]	1.4848 ± 0.0001	1.4803[*]

[*]Extrapolated Value

Temp	Wt. percent	Exptl. Value	Temp	Wt. percent	Exptl. Value
99.2 ± 0.1°C	36.0	1.3073 ± 0.0001	141 ± 0.2°C	53.9	1.4901 ± 0.0001
	43.0	1.3858 ± 0.0001		55.72	1.5160 ± 0.0001
	43.97	1.3969 ± 0.0001		59.71	1.5622 ± 0.0001
	55.4	1.5324 ± 0.0001		65.1	1.6268 ± 0.0001
	59.46	1.5809 ± 0.0001			
120.5±0.1°C	55.4	1.5205 ± 0.0001	161.4±0.1°C	64.68	1.6086 ± 0.0001
	59.46	1.5683 ± 0.0001		72.25	1.7046 ± 0.0001
	65.1	1.6342 ± 0.0001		77.1	1.7652 ± 0.0001

8
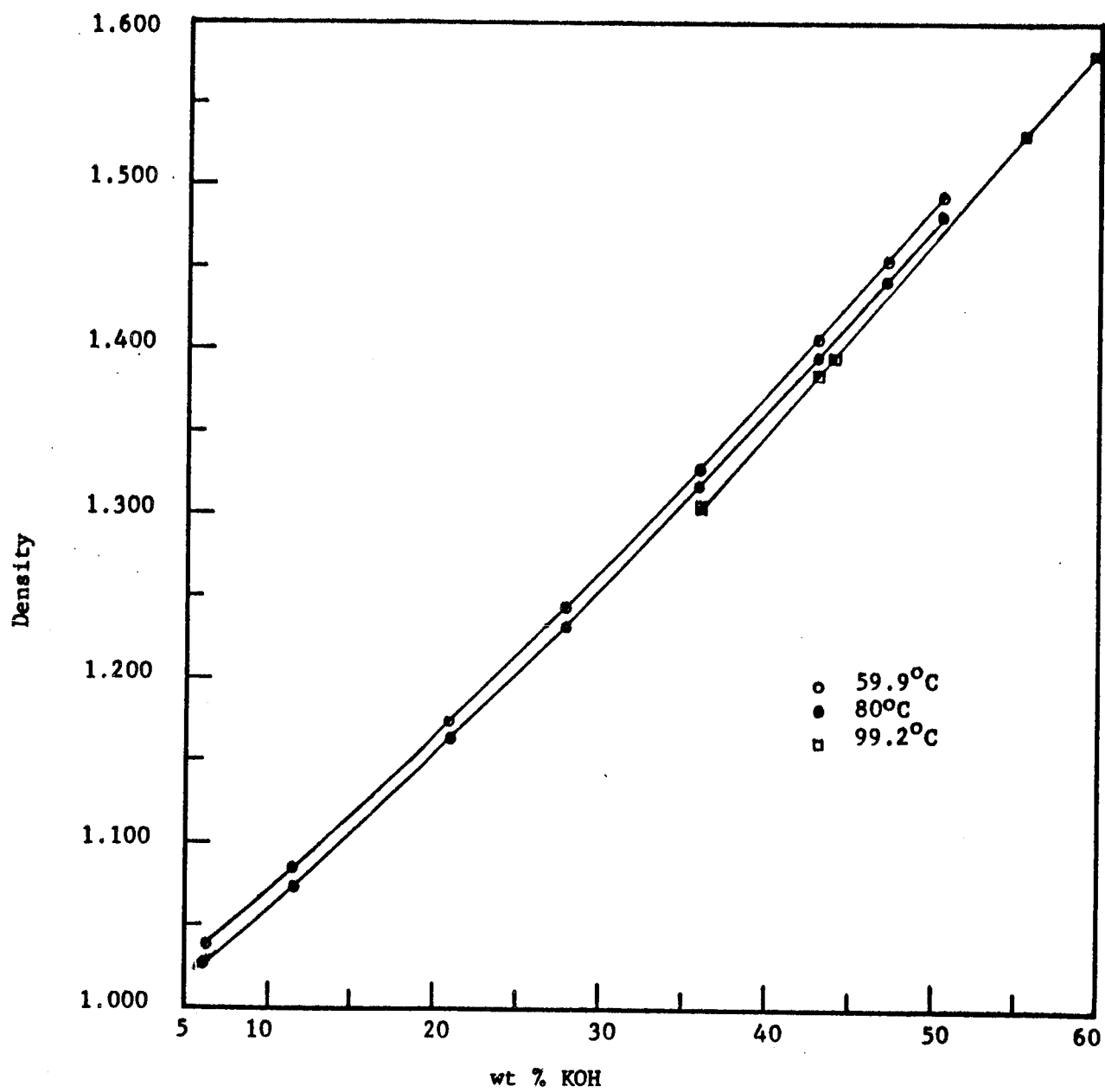
Figure 2

CONCENTRATION DEPENDENCE OF DENSITY OF AQUEOUS KOH SOLUTIONS
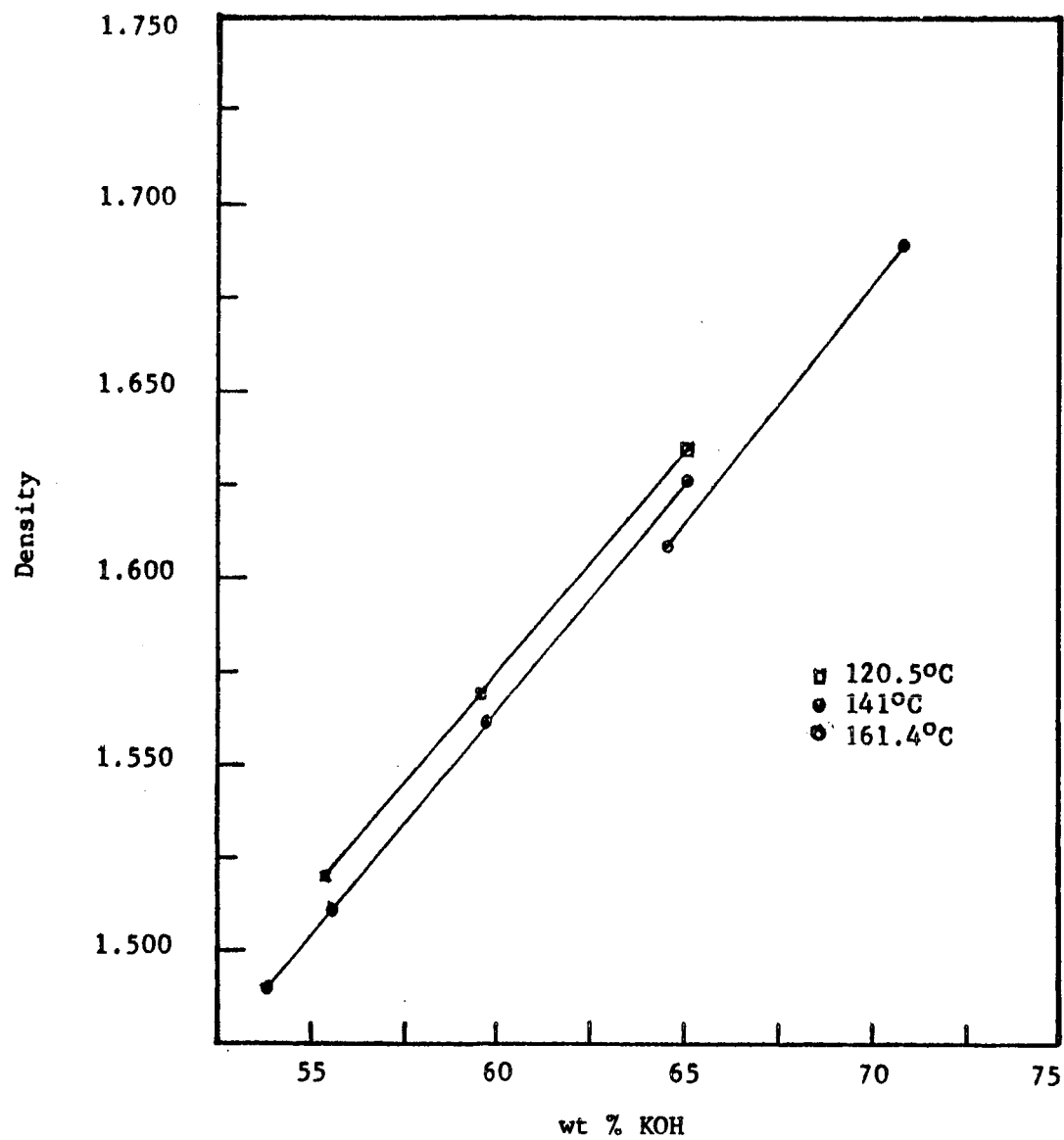
Figure 3

CONCENTRATION DEPENDENCE OF DENSITY OF AQUEOUS KOH SOLUTIONS

deviations shown are standard deviation from the arithmetic means. The error in the concentration determination is estimated to be about 0.1% of the total KOH concentration. No measurements were made of a solution whose vapor pressure were greater than 400mm Hg at a given temperature because it was felt that uncertainty in the measured values that would arise due to rapid vaporization would be too great, and extrapolation from values at low vapor pressure may give better results. The deviations in the temperatures shown in the table represent errors in temperature determination rather than fluctuation in temperature during an experiment.

3.0 VAPOR PRESSURES OF KOH SOLUTIONS

Although the principal object of this work is the measurement
and prediction of solubility and diffusivity of hydrogen and oxygen in
KOH solutions, it is necessary to know the vapor pressure of water at
various temperatures and KOH concentrations. Adequate experimental data
on the vapor pressure of water are not available for the higher values
of temperature and KOH concentration which were planned for investigation
at the outset, and experimental determination of vapor pressures of water
was undertaken both to confirm some of the data in the literature and to
provide those which were unavailable. Since that time, however, interest
appears to have decreased somewhat in the data for higher temperatures
and KOH concentrations, and, with the concurrence of NASA technical
personnel, this particular task was set aside for the time being to con-
centrate more on solubility and diffusivity.

Literature data on vapor pressures over KOH solutions were
tabulated in Section 8.1.5 of the First Semi-Annual Report on Research
Grant NGR 10-005-022. Additional data derived from Duhring lines and
boiling points are summarized in Tables 3.0-1 and 3.0-2. Analysis of
all of these data, including those determined in these laboratories,
suggested that good interpolation and moderate extrapolation could be
obtained from the literature data on vapor pressures over KOH solutions
by means of Antoine equations, provided the empirical constants were
determined carefully. To this end computer evaluation of the constants
was undertaken.

11

Table 3.0-1

VAPOUR PRESSURE OF AQUEOUS KOH SOLUTIONS[4]

(In Millimeters of Mercury)

Wt. % KOH	120°C	140°C	160°C	180°C	200°C	220°C
0	1490	2680	4670	7550	---	---
10	1380	2510	4370	7000	---	---
20	1200	2200	3800	6140	---	---
30	960	1760	3010	5070	7770	---
40	650	1240	2200	3670	5940	---
50	350	650	1150	2020	3270	5300
55	207	380	720	1220	2030	3100

Table 3.0-2

BOILING TEMPERATURES OF AQUEOUS KOH SOLUTIONS AT VARIOUS PRESSURE[4]

				Pressures				
Wt. % KOH	Millimeters of Mercury			Atmospheres				
	100	200	400	1	2	3	5	10
0	52°C	66°C	84°C	100°C	120°C	134°C	152°C	180°C
10	53°C	68°C	85°C	102°C	123°C	136°C	155°C	183°C
20	56°C	71°C	89°C	106°C	127°C	141°C	160°C	189°C
30	62°C	77°C	95°C	113°C	135°C	148°C	168°C	197°C
40	71°C	87°C	106°C	124°C	146°C	161°C	181°C	211°C
50	89°C	106°C	125°C	145°C	168°C	184°C	206°C	273°C
60	115°C	135°C	155°C	178°C	205°C	222°C	246°C	284°C
70	148°C	172°C	198°C	227°C	258°C	280°C	310°C	357°C
80	---	223°C	255°C	287°C	328°C	354°C	387°C	444°C

Correlation of Existing Data.

To correlate existing vapor pressure data for potassium hydroxide
solutions the Antoine equation was used:

$$\log P = A - \frac{B}{C+t} \qquad (3.0-1)$$

where P is vapor pressure in millimeters of mercury, t is temperature in
$^\circ$C, and A, B and C are constants which vary with the KOH concentration.
The experimental data consisted of vapor pressure measurements at tempera-
tures up to 100°C (2), and those based on Duhring lines and boiling temp-
erature data (3,4) at higher temperatures (see Tables 3.0-1 and 3.0-2).
In determining the constants A, B and C for each KOH concentration, the
following procedure recommended by Weissberger (5) was used:

1) The data was plotted as log P vs. 1/(273+t), and inspected for
linearity and scatter in the data points. It was found that the data
could be best represented by two straight lines, corresponding to a
low and high temperature range for each KOH concentration. The transi-
tion temperature from the low to the high temperature region varied
somewhat with concentration, being approximately 60°C for water and
rising to about 120°C at higher KOH concentrations. Two sets of Antoine
constants were subsequently obtained, corresponding to these two regions.

On examining the experimental data a few points were found
which departed somewhat from the straight line in a random fashion.
Where such deviations appeared to be due to experimental error, these
points were not subsequently used in obtaining the constants.

2) For each KOH concentration, values of the constant C were found

for each temperature region from the equation:

$$\frac{\log P - \log P_1}{t - t_1} = \frac{A}{t_1 + C} - \frac{\log P}{t_1 + C} \qquad (3.0\text{-}2)$$

where t_1 is some reference temperature and P_1 is the vapor pressure at that temperature. C was evaluated by plotting the left-hand side of this equation against log P, and determining the slope. Values of C found in this way showed an increase with increasing KOH concentration. Before calculating A and B, the C values were rounded to the nearest degree.

3) Having found values of C for each KOH concentration, the best straight line relating log P to $1/(C+t)$ was determined for both the high and low temperature regions, and hence values of A and B were found by the method of least squares. These calculations were performed on a digital computer.

Values for the constants A, B and C for various KOH concentrations are shown in Table 3.0-3 for the low temperature region, and in Table 3.0-4 for higher temperatures. The values of C obtained show a continuous variation with KOH concentration, but the variations in A and B with concentration are less well-defined. This is attributed to small errors in the experimental vapor pressure data. It seems that several sets of A, B and C values are possible for each concentration, each set giving almost as good a fit of the experimental data; a meaningful choice between these various sets would require vapor pressure data of very high accuracy.

The Antoine equation with the constants shown in Tables 3.0-3 and 3.0-4 gave good agreement with experimental data over the whole range

Table 3.0-3

ANTOINE CONSTANTS FOR LOW TEMPERATURE RANGE

Wt. % KOH[*]	Temperature Range	A	B	C
0	0-80°C	8.0928	1746.1	235
4.72	0-80	8.0757	1745.3	235
9.09	0-80	8.0646	1747.1	235
16.66	0-80	8.1052	1768.1	235
23.07	0-90	7.9800	1751.7	235
28.57	0.100	7.9603	1772.2	236
33.33	0-100	7.9782	1818.7	239
37.50	0-120	8.0529	1891.5	243
44.45	0-120	8.3770	2118.9	254
50.00	0-140	9.5007	2907.8	300
54.55	0-140	9.8749	3289.3	320

* Experimental data taken from reference 2

Table 3.0-4

ANTOINE CONSTANTS FOR HIGH TEMPERATURE RANGE

Wt. % KOH[*]	Temperature Range	A	B	C
0	80-180°C	7.9668	1668.2	228
10	80-180	7.9564	1676.4	228
20	90-180	7.9221	1685.9	228
30	100-200	7.8321	1696.6	230
40	120-200	7.9805	1818.2	232
50	140-220	7.8007	1840.4	234
60	140-250	7.8496	2090.3	243
70	150-310	7.5914	2305.3	264
80	220-440	7.5886	2814.0	303

*Experimental data taken from references 3 and 4

of temperatures and KOH concentrations, the agreement between predicted
and experimental vapor pressures being within 1% for all points. A
comparison of predicted and experimental values for a number of KOH
concentrations and temperatures chosen at random is shown in Table 3.0-5.
Since the agreement in most cases is better than 1%, it is concluded that
the Antoine equation provides estimates of the vapor pressure of KOH
solutions that are sufficiently accurate for the purposes of the work
under this grant.

Table 3.0-5

COMPARISON OF PREDICTED AND EXPERIMENTAL VAPOR PRESSURES

Wt. % KOH	Temperature Range	Temperature °C	P_{predic} mm.Hg	$P_{expt.}$ mm.Hg
23.07	0-100	20	12.9	12.9
		40	40.7	40.7
		60	110.1	110.1
		80	262.4	263
		100	563.6	563
33.33	0-100	40	28.8	28.6
		60	78.6	78.6
		80	189.3	190
		100	410.6	413
44.45	0-100	20	4.40	4.40
		60	42.6	42.6
		80	107.9	108
		100	246.3	246
20.0	100-180	100	606	600
		120	1195	1200
		140	2192	2200
		160	3775	3800
		180	6165	6140
60.0	178-284	178	766	760
		205	1527	1520
		222	2261	2280
		246	3758	3800
		284	7642	7600
80.0	223.444	223	198.6	200
		328	1543	1520
		354	2316	2280
		387	3712	3800
		444	7600	7600

4. SOLUBILITY

4.1 Experimental

As noted in previous reports, the solubility of O_2 in potassium hydroxide solution decreased so sharply with concentration that certain changes were necessary in the apparatus previously described in order to obtain reliable measurements at higher concentrations and temperatures. A new stripping cell was designed in which the glass frit was replaced by a teflon frit, and this was joined to glass pieces by a specially constructed teflon fitting. This was done with a view to preventing corrosion of the frit by KOH at high temperatures and concentrations. The size of the stripping cell was also increased so that larger samples could be injected. Secondly, some changes were made in the saturating system so that as far as possible an absolutely air-free sample could be withdrawn from the saturator. The rest of the apparatus and the experimental procedure has remained essentially the same except that larger samples were injected. In this manner, the reliability of the results was greatly increased although it was noticed that the helium purifier being used presently (adsorption column kept in a liquid nitrogen bath) was not sufficient to remove all the impurities in the helium. It is hoped that this difficulty will be overcome as soon as a gas diffusion helium purifier is secured.

4.2 Results Solubility of O_2 in KOH

The solubility data at 60°C and 100°C obtained after introducing the above described changes in the apparatus are tabulated in Table 4.1-1. These data are also shown in Figure 4, where log S is plotted against weight percent KOH.

18

Table 4.1-1

SOLUBILITY OF O_2 IN KOH

T = 60°C

KOH Concentration Wt. %	O_2 Solubility gmmol/Literx10³
5.56	0.612 ± 0.013
11.22	0.446 ± 0.014
20.9	0.172 ± 0.005
27.8	0.093 ± 0.0015
32.46	0.0614 ± 0.0024
43.97	0.0204 ± 0.0009
51.90	0.0034 ± 0.0013

T = 100°C

38.1	0.0323 ± 0.0011
43.97	0.0173 ± 0.001
56.2	0.00325 ± 0.00027
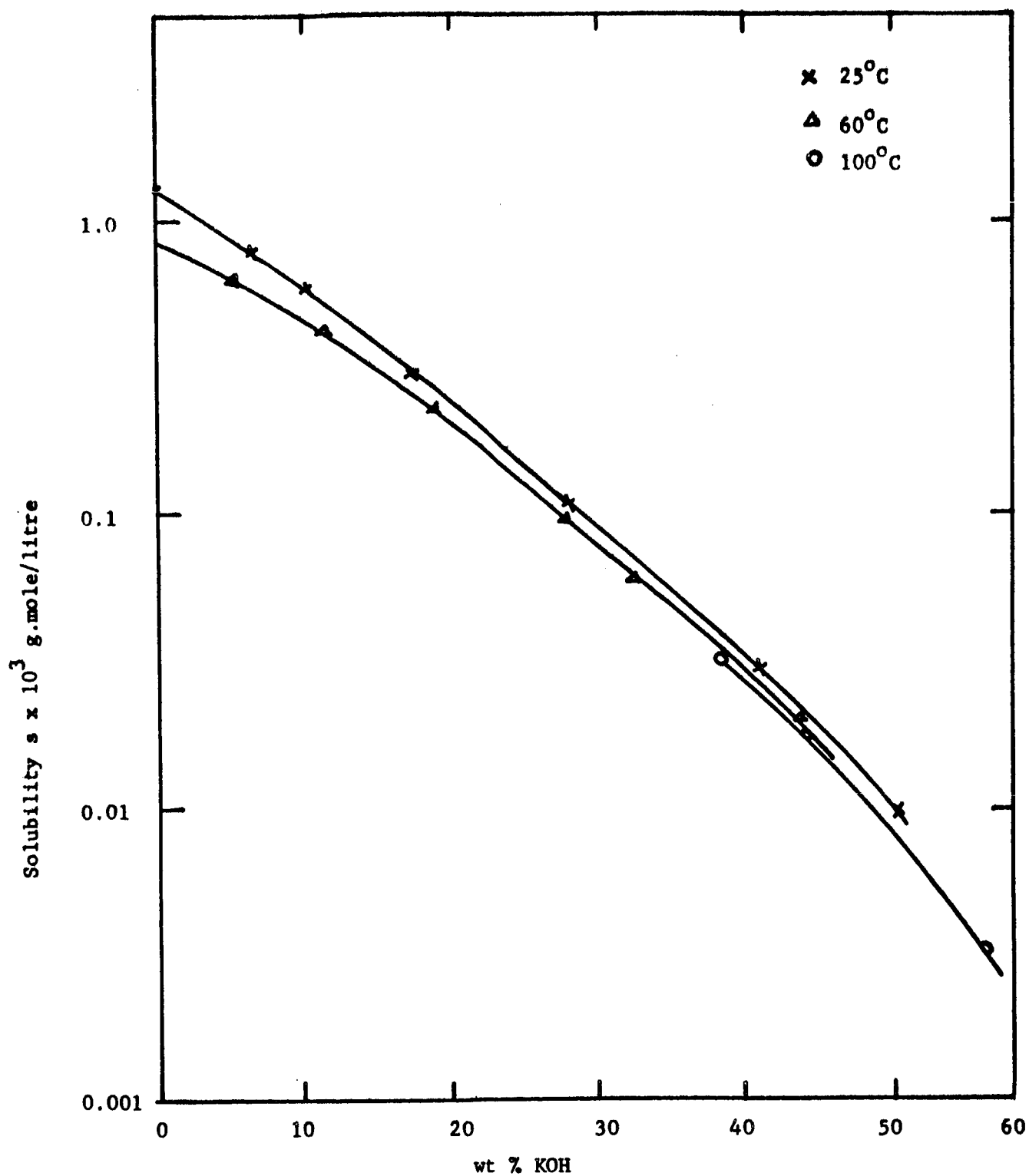
Figure 4

SOLUBILITY OF O_2 IN KOH

4.3 Discussion

4.3.1 Heats of Solution

Since one of the objects of this work is the development of a theory of solution for concentrated electrolytic solutions, it seemed desirable to consider the interactions between the solute molecules (H_2 and O_2) and the solvent. To this end data from Lange (6) for the solubility of hydrogen and oxygen in water at different temperatures were plotted as shown in Figure 5. It may be seen from the graph that the solubility of O_2 in water decreases continuously with increasing temperature whereas that of hydrogen decreases at lower temperatures and then increases at higher temperatures. Thus the solubility of hydrogen in water exhibits a minimum.

These solubility data were used to calculate partial molal heats of solution from the following relation:

$$\left(\frac{\partial \ln x_i}{\partial \frac{1}{T}} \right)_P = \frac{\overline{H}_L^o - \overline{H}_G^*}{R} \qquad (4.3\text{-}1)$$

where x_i = mol fraction of gas

$\quad$ T $\;$ = absolute temperature

$\quad \overline{H}_L^o$ = partial molal enthalpy of the solute in the standard state of infinite dilution

$\quad \overline{H}_G^*$ = partial molal enthalpy of the ideal gas in the vapor phase

$\quad$ R $\;$ = gas constant

$\quad$ P $\;$ = pressure

These values have been tabulated in Table 4.3-1 and plotted in Figure 6. It may be seen from the plots that the partial molal heats of solution for these systems vary considerably with temperature.
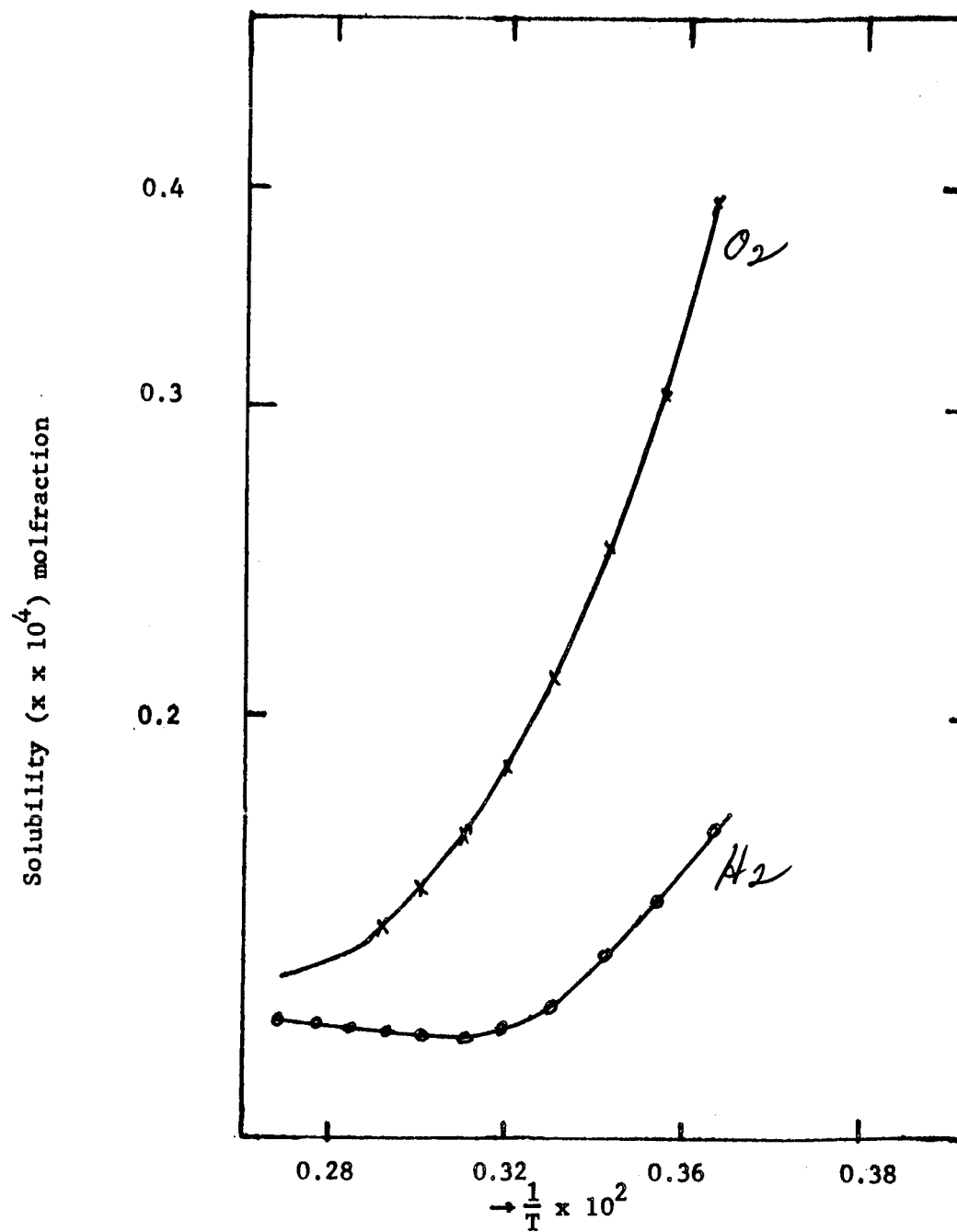
Figure 5

SOLUBILITY OF O_2 AND H_2 IN WATER V_5
RECIPROCAL ABSOLUTE TEMPERATURE

Table 4.3-1

Heats of Solution for O_2/H_2O

Temperature, $^{\circ}$K	ΔH, cal/mol.
283	-3.79×10^3
303	-2.59×10^3
333	-1.28×10^3
363	-0.31×10^3

Heats of Solution for H_2/H_2O

Temperature, $^{\circ}$K	ΔH, cal/mol.
278	-1.45×10^3
294	-1.16×10^3
310	-0.49×10^3
316	-0.18×10^3
323	0
338	0.05×10^3
355	0.06×10^3
373	0.11×10^3
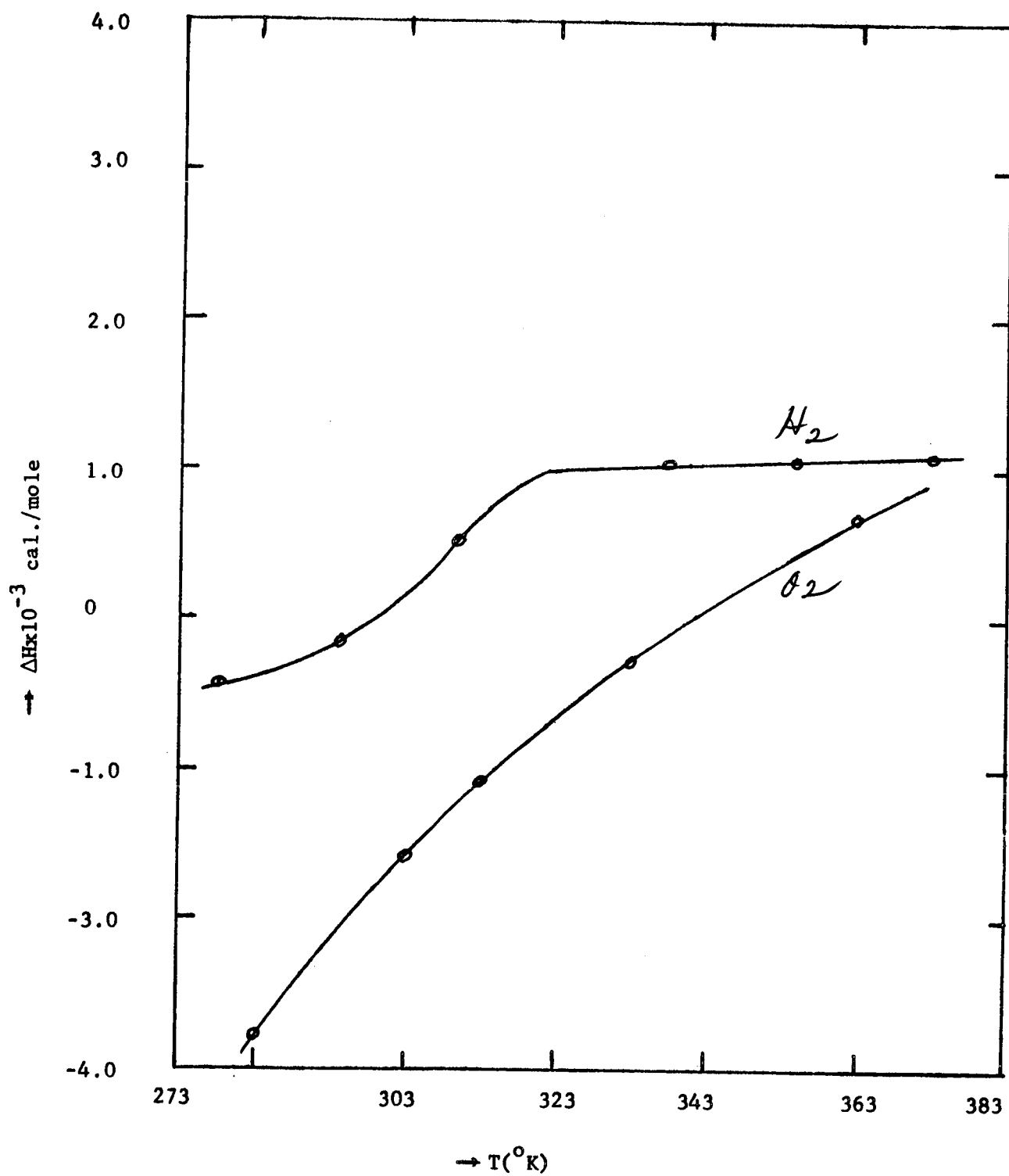
Figure 6

MOLAL HEATS OF SOLUTION (O_2 AND H_2/WATER V_5. ABSOLUTE TEMPERATURE

Since only one solvent is under consideration, namely, water, it is reasonable to assume that differences in the partial molal heats of solution and solubility phenomena are due to the physical characteristics of the gases, or at least, on their effect on the properties of the solvent. Among the common methods used to correlate the partial molal heats of solution are (a) partial molal volumes, (b) force constants and (c) polarizability (7).

The difference between the solubility behavior of these gases in water and nonpolar solvents appears to be partially explainable in terms of the "ice-like" structure (i.e., ordered) of water. The extent of this "ice-like-ness" can be altered by (a) temperature, (b) pressure, and (c) addition of solute. When a gas molecule dissolves it may affect the size and distribution of the ordered aggregates of water molecules. Moreover, one would expect that the larger the solute atom or molecule the greater the effect. Thus, the greater heat of solution of oxygen than that of hydrogen appears reasonable. Furthermore, as the temperature increases the effect on the heat of solution of oxygen is greater as one might expect.

4.3.2 Surface Effects and Solubility

In all work done in these laboratories solutions have been saturated with oxygen by bubbling the gas through a glass frit; a question arose, therefore, as to whether the solubility might be affected by bubble size. In order to investigate the relative importance of surface effects in the solubility measurements, a relation between the solubility of a gaseous solute in a liquid solvent for a curved surface and that for planar surface was derived. The complete derivation from the appropriate

thermodynamical relations has been given in Appendix 1; the final relation is:

$$\frac{x_i^{(c)}}{x_i^{(p)}} = \exp\left(\frac{2\overline{V}_i \sigma}{rRT}\right) \qquad (4.3\text{-}2)$$

where $x_i^{(c)}$ is solubility in case of curved surface

$\quad\quad\;\; x_i^{(p)}$ is solubility in case of planar surface

$\quad\quad\;\; \overline{V}_i$ is partial molal volume of gaseous solute

$\quad\quad\;\; r$ is radius of the bubble

$\quad\quad\;\; R$ is gas constant

$\quad\quad\;\; T$ is absolute temperature

$\quad\quad\;\; \sigma$ is surface tension

The ratio of the solubility on the curved surface to that on the planar surface has been calculated by means of above relation for the O_2/H_2O system. It was found that surface effects were negligible until the bubble radius became as small as 0.001cm.

Consideration of the numerical values of the quantities in equation 4.3-2 suggests that the error will be approximately the same or smaller for strong KOH solutions and/or higher temperatures.

5.0 Mutual Diffusivity of Water in Aqueous KOH Solution

When one is discussing mass transport, it is necessary to specify both the units and the reference frame within which the mass transfer occurs. For a binary system in which diffusion is occurring in one direction only, Fick's first law can be written in the form

$$N_{ix} = - D_{is} \, dC_i/dx \qquad (5.0\text{-}1)$$

where N_{ix} = molar flux of species i diffusing in the x direction, $\dfrac{\text{g.moles}}{\text{cm}^2\text{-sec}}$

D_{is} = diffusivity of species i in solvent system s, $\dfrac{\text{cm}^2}{\text{sec}}$

C_i = molar concentration of species i, $\dfrac{\text{g.moles}}{\text{cm}^3}$

Equation (5.0-1) serves as a defining relation for the diffusion coefficient, D_{is}, and the choice of the symbol N for the flux indicates that a fixed frame of reference has been specified and that the concentration is given in g.moles per unit volume. Strictly speaking equation (5.0-1) is an approximation for the diffusion coefficients of both species are important in principle. However, if both coefficients are equal ($D_{is} = D_{si}$) equation (5.0-1) is satisfactory. One way to insure this is to define flows with respect to a plane across which no net transfer of volume occurs. In this volume fixed reference plane

$$D_1^V = D_2^V = D_{12}^V = D \qquad (5.0\text{-}2)$$

where the subscripts refer to components 1 and 2, respectively. This common coefficient can be termed a mutual diffusion coefficient.

5.1 Experimental

The present work is concerned with the mutual diffusivities of

water in aqueous KOH solutions in the concentration range zero to satura-
ted and temperature from 25°C to 160°C. The method employed was the
standard magnetically stirred diaphragm cell (8) with suitable modifications
owing to the very corrosive nature of the electrolyte solutions. The dia-
phragms used were porous Teflon, Grade G, with an average pore size of 9μ,
and the cell compartments were machined from extruded FEP teflon as shown
in Figure 7.

The experimental method consisted of first evacuating the cell
and drawing degassed distilled water through the diaphragm a number of
times. It was essential to remove all the air from the pores of the dia-
phragm during this process. Also all solutions used were previously
degassed to prevent bubble formation during the experiment. When the
cell was finally filled with distilled water, the vacuum was released
and a hypodermic needle inserted through the upper ℣ joint. The water
was carefully drawn out from the upper compartment and replaced by KOH
solution. For the filling of the stopcock and capillary a hypodermic
syringe with a thin needle was employed. The cell was then inverted and
immersed in a constant temperature bath and diffusion allowed to proceed
for about two hours until steady state concentrations had been attained
in the diaphragm. At this point the solution in the upper compartment
was replaced with fresh distilled water, and the run was timed from this
point. (If large changes of concentration occurred in the KOH solution
in the lower compartment, it was also replaced.) The diffusion was
allowed to proceed for about two days; then the solutions in both the
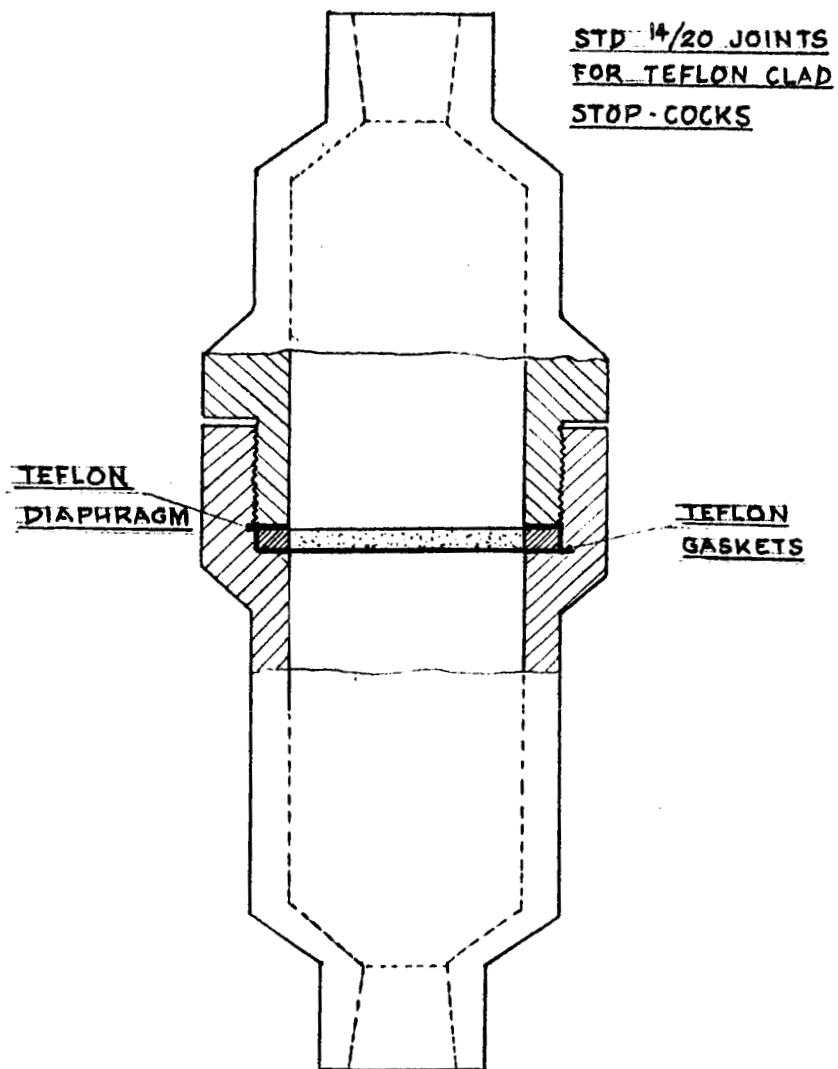compartments were analysed by titration and the integral diffusion

STD 14/20 JOINTS
FOR TEFLON CLAD
STOP-COCKS

TEFLON
DIAPHRAGM

TEFLON
GASKETS

FIGURE 7. DIAPHRAGM CELL (TEFLON FEP)

SCALE: FULL SIZE

coefficient obtained by using the equation

$$\bar{D} = \frac{1}{\beta t} \ln \left(\frac{c_o^i - c_1^i}{c_o^f - c_1^f} \right) \qquad (5.1\text{-}1)$$

where $\bar{D}$ = integral diffusion coefficient

β = the cell constant = $\frac{A}{L} \left(\frac{1}{V_o} + \frac{1}{V_1} \right)$

A = effective area for diffusion

L = effective pore length

t = the time of run

$V_o V_1$ = volume of lower and upper compartments, respectively

$c_o^i, c_o^f, c_1^i, c_1^f$ = the initial and final concentrations of the lower and upper compartments, respectively.

The cell calibration to determine β was carried out using KCl solutions for which D is known as a function of concentration from absolute measurements (9). The cell and diaphragm volumes were determined by a series of cell weighings with a liquid of known density.

The KOH used in these measurements contained less than 0.02% carbonate, and was approximately 99.96% pure.

5.2 Method of Calculating Differential Diffusivities

The diffusion coefficient calculated from the diaphragm cell experiments is a rather complicated double average, which it is not easy to convert immediately to the more fundamental differential diffusion coefficient. It has been shown by Gordon(8) that a negligible error is introduced in all ordinary cases if instead of using the exact relation

$$\bar{D} = \frac{1}{t} \int_0^t \bar{D}(t)dt \qquad (5.2\text{-}1)$$

we treat the integrand as having a constant value equal to its value when the concentrations in the two compartments are midway between their initial and final values. This constant value is then equal to $\bar{D}$ as defined above and is related to the differential diffusion coefficient by

$$\bar{D} = \frac{1}{C_m{}'C_m{}''} \int_{C_m{}''}^{C_m{}'} D \, dC \qquad (5.2\text{-}2)$$

where $C_m{}' = \dfrac{C_o^i + C_o^f}{2}$

$ C_m{}'' = \dfrac{C_1^i + C_1^f}{2}$

The problem of computing the D values at various values of concentrations for a set of $\bar{D}$ values obtained in experiments was attempted using Stokes' (11) method. Essentially, this consists of assuming a suitable analytical expression with arbitrary coefficients for D as a function of C, and then determining coefficients so that Equation (5.2-2) above will fit the desired $\bar{D}$ values.

5.3 Volume Change on Mixing

If there is no volume change on mixing during the diffusion process, the volume on either side of the apparatus-fixed reference plane will be unchanged, and this reference plane will be identical with that defined earlier. The condition of zero volume change is fulfilled exactly if the partial molar volume of each component is independent of concentration. Under these circumstances the experimental differential diffusion coefficient will be identical with D_{12}^V. For the KOH-water system, the above condition is not exactly fulfilled; however, we present calculations below to prove that the correction due to volume changes is negligible. For

this we employ the method of Olander (12) who developed an equation from which it can be quickly ascertained whether the volume change corrections are necessary for a particular system or not. From his Equation (14) we have

$$\bar{D}\left[\frac{1-AG}{1-r\langle\bar{V}_s\rangle\delta_o}\right] = D_o + \sum_{j=1}\zeta_i\left[\frac{1-\left(r\langle\bar{V}_s\rangle\delta_j\right)/\zeta_j}{1-r\langle\bar{V}_s\rangle\delta_o}\right]a_j \qquad (5.3\text{-}1)$$

where $\bar{D}$ = measured integral diffusion coefficient

$$\equiv \frac{1}{\beta t}\ln(\theta_i/\theta_f)$$

$$\theta = C_o - C_1$$

A = a parameter in Olander's Eqn. (10)

$$= r\bar{V}_{sb} \text{ when } C_1^i = 0$$

$$G = \frac{2\left(C_o^i+C_1^i\right)\left(\theta_i-\theta_f\right) - \frac{3}{2}\left(\theta_i^2-\theta_f^2\right) + \theta_i^2\ln\left(\theta_i/\theta_f\right)}{4\ln\left(\theta_i/\theta_f\right)}$$

$\langle\bar{V}_s\rangle$ = average value of solvent molar volume between upper and lower compartments

$$\delta_j = C_o^m\zeta_{j+1} - \zeta_{j+2}$$

D_o = diffusivity at infinite dilution, or Nernst limiting value

$$\zeta_j = \frac{\left(C_o^m\right)^{j+1} - \left(C_1^m\right)^{j+1}}{\left(j+1\right)\left(C_o^m - C_1^m\right)}$$

a_j = coefficients for the expansion when the differential diffusion coefficient is expressed as a power series in C(Olander, Eqn. 13).

Subscripts: o refers to lower compartment

1 refers to upper compartment

Superscripts: i refers to inditial conditions

f refers to fiñal conditions

m refers to mean conditions

The quantity r is given by

$$\overline{V}_{KOH} \Big/ \overline{V}_{H_2O} = k + rC \qquad\qquad c_1^i \leq c \leq c_o^i \qquad\qquad (5.3-2)$$

i.e., r is the slope of the line resulting from a plot of the ratio $\left(\overline{V}_{KOH} \Big/ \overline{V}_{H_2O}\right)$ versus concentration, and k is a constant.

For the case $C_1^i = 0$

$$A = r\overline{V}_{sb} \qquad\qquad (5.3-3)$$

where $\overline{V}_{sb}$ is defined by

$$1 \Big/ \overline{V}_{H_2O} = 1 \Big/ \overline{V}_{sb} + QC \qquad\qquad c_o^i \geq c \geq c_1^i \qquad\qquad (5.3-4)$$

where Q is a constant (Olander Eqn. 7).

From Equation (5.3-1) it is only necessary to evaluate the bracketed terms for an experiment which involves the largest driving force in the region of largest r. If these differ from unity by the same order as the experimental precision, then the correction due to volume changes would be barely significant.

Using the apparent partial molal volume data of Akerlof and Bender (13), the ratio $\overline{V}_{KOH} \Big/ \overline{V}_{H_2O}$ vs. concentration was plotted; also $1/\overline{V}_{H_2O}$ vs. concentration. From these $\langle r \rangle$ and $1/\overline{V}_{sb}$ were found to be 0.1075 liters/g.mole and 80 g.mole liter^{-1}. We shall apply these to the following values obtained for a run:

$$C_o^i = 5.532 \text{ g.mole/liter} \qquad\qquad C_1^i = 0$$

$$c_o^f = 4.174 \text{ g.mole/liter} \qquad\qquad c_1^f = 1.396 \text{ g.mole/liter}$$

$$\theta_i = c_o^i - c_1^i = 5.532 \text{ g.mole/liter}$$

$$\theta_f = c_o^f - c_1^f = 2.778 \text{ g.mole/liter}$$

$$\bar{D} = \frac{1}{\beta t} \ln\left(\frac{c_o^i - c_1^i}{c_o^f - c_1^f} \right) = \frac{1}{(0.184)(50.5)(3600)} \ln \frac{5.532}{2.778} = 2.055 \times 10^{-5} \text{cm}^2 \text{sec}^{-1}$$

$$G = \frac{2\left(c_o^i + c_1^i \right)\left(\theta_i - \theta_f \right) - 3/2\left(\theta_i^2 - \theta_f^2 \right) + \theta_i^2 \ln\left(\theta_i / \theta_f \right)}{4\ln(\theta_i / \theta_f)}$$

$$G = \frac{2(5.532 + 0)(5.532 - 2.778) - (3/2)\left[(5.532)^2 - (2.778)^2 \right] + (5.532)^2 \ln(5.532/2.778)}{4\ln(5.532/2.778)}$$

$$= 6.24978$$

$$c_o^m = (1/2)\left(c_o^i + c_o^f \right) = 4.853 \text{ g.mole/liter}$$

$$c_1^m = (1/2)\left(c_1^f + c_1^f \right) = 0.698 \text{ g.mole/liter}$$

$$\zeta_1 = (1/2)\ c_o^m + c_1^m = 2.7755$$

$$\zeta_2 = (1/3)\left[\left(c_o^m \right)\left(c_1^m \right) + \left(c_1^m \right)^2 \right] = 9.143$$

$$\delta_o = c_o^m\ \zeta_1 = \zeta_2 = 4.3266$$

$$\left\langle \bar{v} \right\rangle = \left\langle \bar{v}_{H_2O} \right\rangle = 17.8 \text{ ml} = 0.0178 \text{ liters}$$

For this case, since $c_1^i = 0$

$$A = r\bar{V}_{sb} = (0.001344)$$

$$\left[\frac{1 - AG}{1 - r\langle\bar{v}\rangle\delta_o} \right] = \left[\frac{1 - 0.0084}{1 - (0.1075)(0.0178)(4.3266)} \right] = 0.9988$$

Also $\left[\dfrac{1-r\langle\overline{V}\rangle\delta_1/\zeta_1}{1-r\langle\overline{V}\rangle\delta_o} \right] = \left[\dfrac{1-0.0097}{1-0.0083} \right] = 0.9986$

Since both the bracketed terms differ from unity by very small factors the correction due to volume changes is therefore insignificant. Because the above calculation was performed for the case for which volume changes should be most significant, it is concluded that in all cases the volume change effects will be negligible for KOH solutions.

5.4 Experimental Mutual Diffusion Coefficients

The integral diffusion coefficients at 25°C for a few KOH solutions diffusing into water have been obtained and are shown in Table 5.4-1.

Table 5.4-1

INTEGRAL DIFFUSION COEFFICIENTS FOR WATER DIFFUSING IN KOH SOLUTIONS

	c_o^i	c_1^i	c_o^f	c_1^f	$\overline{D}$, cm^2/sec
1	0.96845	0	0.7174	0.2583	2.32×10^{-5}
2	0.9840	0	0.7394	0.2521	2.19×10^{-5}
(i)	10.86819	0	8.3899	2.5498	1.93×10^{-5}
(ii)	10.91935	0	8.52748	2.46091	1.83×10^{-5}

A sample calculation of $\overline{D}$ for an approximately 5% KOH solution diffusing into pure water is shown in Appendix 2.

6.0 Diffusivities of Hydrogen and Oxygen in KOH Solutions

Although these measurements are a principal concern in this work, no experiments were done during this period as all efforts were directed toward getting other data which are necessary. Work in this area will be instituted in the very near future.

7.0 Future Plans

After careful consideration of the area of greatest NASA interest and the technical problems involved in making accurate measurements of physical and transport properties, it has been concluded, with the concurrence of NASA technical personnel, that chief attention should be given to obtaining these data for temperatures below $160^{o}C$ and for KOH concentrations up to 60 wt. percent before attempting work at higher temperatures and KOH concentrations. Therefore, plans for the next six months have been revised. These now include the following:

1. Completion of the measurements of the solubility of hydrogen and oxygen in KOH.

2. Development of theoretical models for solubility of hydrogen and oxygen in KOH based on statistical mechanics.

3. Measurement of the diffusivity of hydrogen and oxygen in KOH solutions.

In respect to item 1 above, it may be worth noting that the limiting factor in making solubility measurements now is the degree to which the helium stripping gas can be purified. In short, the solubility of oxygen has become so low at high temperatures and high KOH concentrations that the impurities remaining in the helium stripping gas after purification are a significant fraction of the dissolved oxygen in a sample. Efforts are being made to further purify the helium, and it is expected that sufficient success will be achieved to enable us to make the necessary measurements at high KOH concentrations and the higher temperatures.

37

Diffusivity measurements with the diaphragm cell (described in earlier reports) also require purer helium because the dissolved gas concentration in these solutions is even less than in the saturated solutions which are used for solubility measurements.

The only work planned on physical properties of KOH solutions is that which is required for making the solubility and diffusivity measurements.

REFERENCES

1. Reddlich, O. and Bigeleisen, J., J. Am. Chem. Soc. <u>64</u>, 758 (1942).

2. International Critical Tables, Volume 4, p. 238 (1928).

3. "Caustic Potash", Solvay Technical and Engineering Service Bulletin No. 15, Solvay Process Division, Allied Chemical Corp., 1960.

4. Gerlach, G. T., Zeit, Anal. Chemie, <u>26</u>, 413 (1887).

5. Thomson, G. W., "Determination of Vapor Pressure", in "Technique of Organic Chemistry", Vo. 1, Part 1, ed. A. Weissberger, 1959.

6. Lange, N. A, Handbook of Chemistry.

7. Himmelblau, D. M., J. Phys. Chem., <u>63</u>, 1803 (1959).

8. Gordon, A. R., Ann. N.Y. Acad. Science <u>46</u>, 285 (1945).

9. Harned, H. S. and Nuttall, R. L., J. Am. Chem. Soc. <u>69</u>, 736 (1947); <u>71</u>, 1460 (1949).

10. Gosting, L. J., J. Am. Chem. Soc. <u>72</u>, 4418 (1950).

11. Stokes, R. H., J. Am. Chem. Soc. <u>72</u>, 2243 (1950).

12. Olander, D. R., J. Phys. Chem. <u>67</u>, 1011 (1963).

13. Akerlof, G., and Bender, P., J. Am. Chem. Soc., <u>63</u>, 1085 (1941).

Appendix 1

Surface Effect and Solubility

Intuitively, it is seen that the pressure inside a bubble is higher than outside on the plane surface, i.e., the chemical potential inside is higher than outside. Quantitatively, the equation for the energy change is:

$$dF = -SdT + VdP + \sigma dA_s + \Sigma \mu_i^{(p)} dn_i \tag{1}$$

The above equation is valid for curved surfaces under the assumptions (i) the surface tension is unchanged by the curvature (ii) the interface within the system does not change the pressure on the exterior. It may be noted that the chemical potential $\mu_i^{(p)}$ in the above equation pertains to transfer of matter which does not change surface area, i.e.

$$\mu_i^{(p)} = \left(\frac{\partial F}{\partial n_i} \right)_{T,P,A_s,n_j} \tag{2}$$

For a spherical bubble, however, the area will change according to the transfer of matter. Thus the volume change on addition of increments dn_i moles of the various components is:

$$dV = \Sigma \bar{V}_i dn_i \tag{3}$$

where $\bar{V}_i$ is partial molal volume of species i.

For a spherical bubble:

$$dA_s = 2 \frac{dV}{\gamma}$$

$$= 2 \Sigma \frac{\bar{V}_i}{r} dn_i \tag{5}$$

Thus, for transfer from a curved surface, we can write

$$dF = -SdT + VdP + \sigma\left(2\ \Sigma\ \frac{V_i}{r}\ dn_i\right) + \Sigma\ \mu_i^{(p)}dn_i \qquad (6)$$

$$= -SdT + VdP + \sum_i\left(\mu_i^{(p)} + 2\ \frac{V_i\sigma}{r}\right)dn_i \qquad (7)$$

We note, therefore, that the chemical potential for a curved surface is raised by an amount $2\dfrac{V_i\sigma}{r}$ over the plane surface chemical potential $\mu_i^{(p)}$ due to surface effects.

The chemical potential for a curved surface, $\mu_i^{(c)}$ is given by:

$$\mu_i^{(c)} = \mu_i^{(p)} + 2\ \frac{\overline{V}_i\sigma}{r} \qquad (8)$$

Now for solubility of gases (O_2 and H_2) in liquids (KOH), equilibrium exists between the gaseous and liquid phases:

$$\mu_i^{g} = \mu_i^{l} \qquad (9)$$

where μ_i^{g} and μ_i^{l} are chemical potentials in the gaseous and liquid phases, respectively.

But, for the case where there are no surface effects

$$\mu_i^{g} = \mu^{o} + RT\ \ln f_i \qquad (10)$$

where $\mu^{o} = f(T)$ only.

$$\mu_i^{l} = \mu^{*} + RT\ \ln \gamma_i x_i^{(p)} \qquad (11)$$

where $x_i^{(p)}$ denotes mole fraction in case of plane surface

and

$$\mu^{*} = f(T,P)$$

$$V_i = f(T,P,x_j^{l})$$

41

On equating Equations (10) and (11) we obtain

$$RT \ln \frac{\gamma_i x_i^{(p)}}{f_i} = \mu^o - \mu^* \tag{12}$$

and

$$x_i = f_i \exp\left(\frac{\mu^o - \mu^*}{RT}\right) \tag{13}$$

Now in case of surface effects

$$\mu_i^g = + \mu_i^{(p)} + 2 \frac{\bar{V}_i \sigma}{r} \tag{14}$$

$$= \mu^o + RT \ln f_i + 2 \frac{\bar{V}_i \sigma}{r} \tag{15}$$

As before by (9), (11) and (15)

$$x_i^{(c)} = \frac{f_i}{V_i} \exp\left[(\mu^o - \mu^*)/RT + 2\bar{V}_i \frac{\sigma}{rRT}\right] \tag{16}$$

where $x_i^{(c)}$ is mole fraction in case of curved surface.

From (13) and (16) we have then

$$\frac{x_i^{(c)}}{x_i^{(p)}} = \exp\left(\frac{2\bar{V}_i \sigma}{rRT}\right) \tag{17}$$

Sample Calculation:

O_2/Water System:

$\sigma = 79.7$ dynes/cm for H_2O

$\bar{V}_{O_2} = 32.00$ cc/mole

$R = 1.987$ cal/g.mole^{o}K $= 4.185 \times 10^7 \times 1.987$, erg/g.mole^{o}K

$T = 298^o$K

42

$$+2\left(\frac{\overline{V}_{O_2}\sigma}{rRT}\right) = \frac{+2 \times 32 \times 79.7}{r \times 4.185 \times 10^7 \times 1.987 \times 298}$$

$$= \frac{2.06 \times 10^{-7}}{r}$$

$$\frac{x^{(c)}}{x^{(p)}} = \exp\left(\frac{2.06 \times 10^{-7}}{r}\right)$$

Take $r = 0.1$ cm

$$\frac{x^{(c)}}{x^{(p)}} = \exp\left(\frac{2.06 \times 10^{-7}}{0.1}\right) = \exp\left(2.06 \times 10^{-6}\right) = 1.0007$$

% Error $= 0.0007 \times 100 = 0.07\%$

Radius of bubble r, cm	% Error in solubility
0.1	0.07
0.01	0.49
0.001	4.66

Appendix 2

Sample Calculations of Mutual Diffusion Coefficients

A. Cell Volumes: Plexiglass Cell No. 1

V_0 = 44.975 ml = volume of lower compartment

V_1 = 43.70 ml = volume of upper compartment

V_2 = 0.95 ml = volume of diaphragm

B. Determination of Cell Constant, β:

10 ml sample from each compartment titrated with $0.1 N A_g NO_3$ soln.

Titration reading from lower compartment = 4.57 ml

Titration reading from upper compartment = 1.39 ml

Then

c_0^f = 0.0457 g.mole/liter $\qquad\qquad$ c_1^f = 0.0139 g.mole/liter

c_1^i = 0

$c_0^i = c_0^f + c_1^f - c_1^i \left(\dfrac{V_1 + 1/2 V_2}{V_0 + 1/2 V_2} \right)$

c_0^i = 0.0592 g.mole/liter

$C_m' = \dfrac{c_0^i + c_0^f}{2}$ = 0.05245 g.mole/liter

$C_m'' = \dfrac{c_1^i + c_1^f}{2}$ = 0.00695 g.mole/liter

$\bar{D}_0(C_m')$ = 1.89x10-5 cm^2/sec

$\bar{D}_0(C_m'')$ = 1.94x10^{-5} cm^2/sec

$\bar{D} = \left[\bar{D}(C_m') - \dfrac{C_m''}{C_m'} \bar{D}_0(C_m'') \right] \bigg/ \left(1 - \dfrac{C_m''}{C_m'} \right)$

$\bar{D}$ = 1.88309x10^{-5} cm^2/sec

t = 49.25 hours

$$\text{Cell constant } \beta = \frac{1}{Dt} \ln \left(\frac{C_o^i - C_1^i}{C_o^f - C_1^f} \right)$$

$$= \left(\frac{1}{1.88309 \times 10^{-5}} \right) \left(\frac{1}{49.25 \times 3600} \right) \ln \left(\frac{0.0592}{0.0457 - 0.0139} \right)$$

$$\beta = 0.186$$

C. Mutual Diffusion Coefficient in Approximately 5 wt. % KOH:

After a run of 48 hours 5 ml samples from each compartment titrated with 1.0N HCl

Bottom compartment 35.87 ml

Top compartment 12.92 ml

Then $C_o^f = 0.7174$ g.mole/liter $\qquad$ $C_1^f = 0.2583$ g.mole/liter

$$C_o^i = C_o^f + \left(C_1^f - C_1^i \right) \left(\frac{V_1 + 1/2V_2}{V_o + 1/2V_2} \right) = 0.9685 \text{ g.mole/liter}$$

$$\bar{D} = \frac{1}{\beta t} \ln \left(\frac{C_o^i - C_1^i}{C_o^f - C_1^f} \right)$$

$$\bar{D} = 2.32 \times 10^{-5} \text{ cm}^2/\text{sec.}$$